Cell PRESS
Developmental Cell
Short Article

Kibra Is a Regulator of the Salvador/Warts/Hippo Signaling Network

Alice Genevet,[1] Michael C. Wehr,[1] Ruth Brain,[2] Barry J. Thompson,[2,*] and Nicolas Tapon[1,*]
[1]Apoptosis and Proliferation Control Laboratory
[2]Epithelial Biology Laboratory
Cancer Research UK, London Research Institute, 44 Lincoln's Inn Fields, London WC2A 3PX, UK
*Correspondence: barry.thompson@cancer.org.uk (B.J.T.), nicolas.tapon@cancer.org.uk (N.T.)
DOI 10.1016/j.devcel.2009.12.011

SUMMARY

The Salvador (Sav)/Warts (Wts)/Hippo (Hpo) (SWH) network controls tissue growth by inhibiting cell proliferation and promoting apoptosis. The core of the pathway consists of a MST and LATS family kinase cascade that ultimately phosphorylates and inactivates the YAP/Yorkie (Yki) transcription coactivator. The FERM domain proteins Merlin (Mer) and Expanded (Ex) represent one mode of upstream regulation controlling pathway activity. Here, we identify Kibra as a member of the SWH network. Kibra, which colocalizes and associates with Mer and Ex, also promotes the Mer/Ex association. Furthermore, the Kibra/Mer association is conserved in human cells. Finally, Kibra complexes with Wts and *kibra* depletion in tissue culture cells induces a marked reduction in Yki phosphorylation without affecting the Yki/Wts interaction. We suggest that Kibra is part of an apical scaffold that promotes SWH pathway activity.

INTRODUCTION

Growth regulation is a critical developmental process whose dysfunction can lead to many diseases, including cancer (Conlon and Raff, 1999). The Salvador (Sav)/Warts (Wts)/Hippo (Hpo) (SWH) network, identified in *Drosophila* and conserved in mammals, plays a major role in limiting growth by inhibiting cell proliferation and promoting apoptosis (Harvey and Tapon, 2007; Reddy and Irvine, 2008). Activation of the upstream kinase Hpo allows it to phosphorylate the downstream kinase Wts, which in turn phosphorylates and inhibits the transcription coactivator Yorkie (Yki). Scaffold proteins, such as Salvador (Sav) and Mats, potentiate the activity of the Hpo/Wts complex (Harvey and Tapon, 2007). One upstream input of the pathway is mediated via Merlin (Mer) and Expanded (Ex), two FERM (Four point one, Ezrin, Moesin, Radixin) domain proteins (Hamaratoglu et al., 2006). Recently, Ex was shown to bind Yki, and new experiments hint at the existence of an Ex/Hpo/Wts-containing apical complex anchoring Yki at the cortex (Badouel et al., 2009; Oh et al., 2009). These findings underline the importance of scaffold proteins in the regulation of the pathway. However, though some upstream members are known, how the SWH network is activated remains unclear.

Here, we identify the WW-domain-containing protein Kibra as a regulator of the SWH network. Human KIBRA (Kremerskothen et al., 2003) is known to be phosphorylated by Protein Kinase C ζ (PKCζ) (Buther et al., 2004) and has recently been reported to have a role in cell migration (Duning et al., 2008; Rosse et al., 2009). In *Drosophila*, Kibra had previously been recovered as a minor hit in several screens for growth regulators (Boutros et al., 2004; Muller et al., 2005; Ringrose et al., 2003; Tseng and Hariharan, 2002) but has not been further studied. Our experiments show that Kibra associates with Mer, Ex, and Wts and stabilizes the Mer/Ex interaction. This suggests that Kibra is a component of an apical scaffold that controls SWH pathway activation.

RESULTS

kibra and *wts* RNAi Depletion Induce Similar Overgrowth Phenotypes

We performed an in vivo screen in the fly wing in order to identify genes implicated in growth control. Transgenic flies bearing RNA interference (RNAi) constructs generated by the Vienna *Drosophila* RNAi Centre (VDRC) (Dietzl et al., 2007) were crossed to the *hedgehog-GAL4* (*hh-GAL4*) driver, leading to target gene silencing in the posterior compartment of the wing. We screened a collection of 12,000 lines targeting genes conserved between *Drosophila* and mammals. The results of this screen will be described elsewhere.

In this context, expressing an RNAi line directed against *kibra* induced overgrowth of the posterior wing compartment (Figure 1B) compared to control flies (Figure 1A). This phenotype was also observed upon *wts* depletion (Figure 1C). Driving the same *kibra* RNAi line in the eye also led to increased organ size (Figures 1D and 1E), similarly to a *wts* RNAi line (Figure 1F). To exclude off-target effects, we generated a transgenic line expressing a nonoverlapping RNAi construct and observed identical overgrowth phenotypes (data not shown). Furthermore, adult eye sections revealed that *kibra* knockdown retinas present an excess of interommatidial cells (IOCs) (Figures 1G and 1H). The IOCs, the last population of cells to differentiate in the eye primordium, give rise to the secondary and tertiary pigment cells that optically isolate the ommatidia in the compound eye from each other. Extra IOCs are produced during normal development but are then eliminated by apoptosis at the pupal stage to give rise to the adult lattice (Wolff and Ready, 1993). The presence of extra IOCs is a hallmark of SWH network loss of function (Kango-Singh et al., 2002; Tapon et al., 2002), which reduces

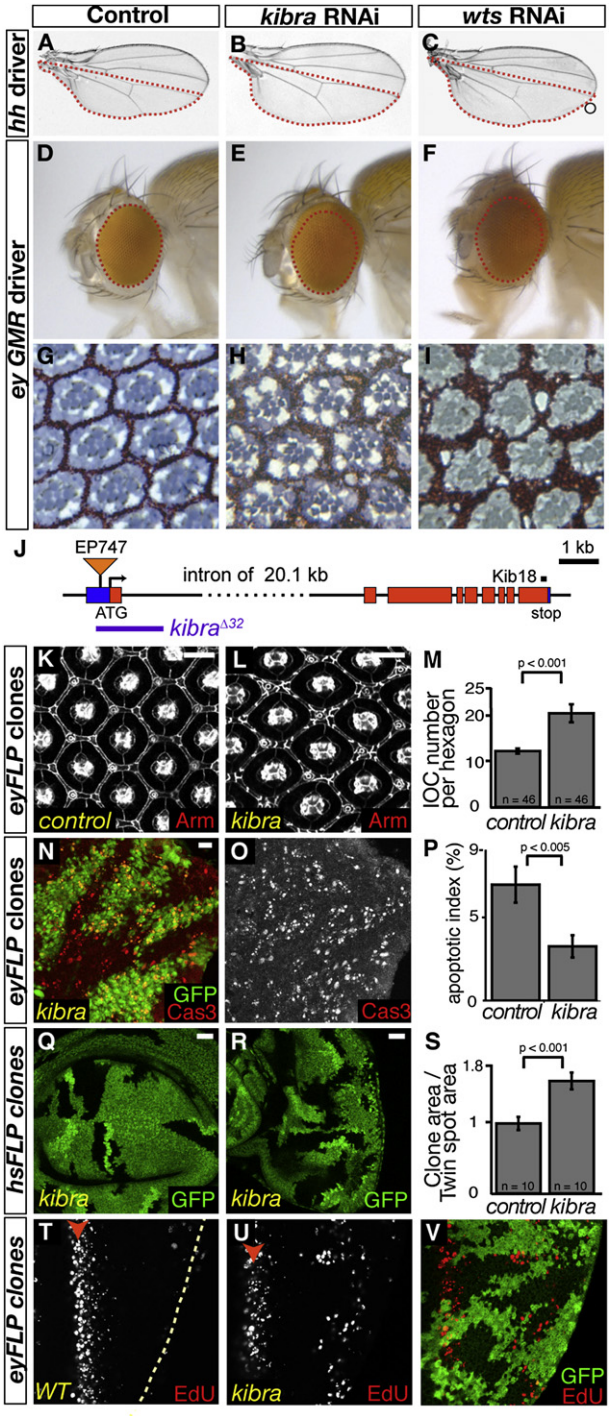

Figure 1. Kibra Loss of Function Induces a Phenotype Similar to SWH Network Loss of Function

(A–C) Control wings (A) and wings where the *kibra* (B) or *wts* (C) genes were silenced by RNAi in the posterior compartment (red dotted line).

(D–I) Control fly eyes (D and G) and eyes expressing the same RNAi lines against *kibra* (E and H) or *wts* (F and I). In adult eye sections (G–I), interommatidial cells (IOCs) are in red and photoreceptors in blue.

(J) Schematic of the *kibra* locus showing the localization of the $kibra^{\Delta 32}$ allele, generated by excision of the *EP747* P element (triangle). The coding sequence is in red; 5′- and 3′-UTRs are in blue. In black is the peptide recognized by the Kib18 antibody.

(K–M) 40 hr APF retinas containing *kibra* mutant clones. (K and L) Cell outlines are visualized by anti-Arm staining (scale bar = 10 μm). (M) Quantification of the IOCs. The p value from a Mann-Whitney test is shown.

(N–P) Apoptotic index in 28 hr APF retinas containing *kibra* mutant clones (absence of GFP). A retina stained for activated Caspase-3 (Cas3) merged with GFP is shown in (N). The Cas3 staining for the whole retina is shown in (O). (P) Quantification of the apoptotic index. The p value from a Mann-Whitney test is shown.

(Q–S) Wing disc (Q) and eye disc (R) containing *kibra* clones (lack of GFP). Scale bars = 20 μm. (S) Quantification of the proliferation advantage of WT or *kibra* mutant cells by calculating the ratio between total clonal area (no GFP) and total twin spot area (two copies of GFP) for discs containing either WT or *kibra* clones. The p value from a Mann-Whitney test is shown.

(T–V) EdU labeling (shown in gray or red) of WT discs (T) and of discs containing *kibra* clones (U and V). Posterior is to the right, and the SMW is indicated by a red arrowhead. See also Figure S1.

Error bars represent standard deviations.

retinal apoptosis, as seen in *wts* RNAi adult eye sections (Figure 1I). Thus, depletion of *kibra* elicits a similar phenotype to SWH network mutants, suggesting a potential role for Kibra in Hpo signaling.

kibra Loss of Function Causes Excess Proliferation and a Reduced Apoptotic Rate, Similarly to SWH Network Loss of Function

To study *kibra* loss of function, we generated the $kibra^{\Delta 32}$ allele by imprecise excision of the *EP747* transposon (see Figure 1J and Experimental Procedures). This deletion allele, which removes the translation initiation site, is homozygous lethal and may be a null allele for *kibra*. $kibra^{\Delta 32}$ FLP/FRT mutant clones in 40 hr after-puparium-formation (APF) retinas present extra IOCs (Figure 1K–1M), similarly to what was observed in adult eyes with *kibra* knockdown (Figures 1G–1I). Duplication of bristles or missing bristles can also be observed. We determined apoptotic indexes (Colombani et al., 2006) during the retinal apoptosis wave (28 hr APF) in pupal retinas containing *kibra* mutant clones stained with an anti-active Caspase-3 antibody. *kibra* mutant tissue presents a reduced apoptotic index compared with *wild-type* (WT) areas in the same retinas (Figures 1N–1P; see Figures S1A–S1A‴ available online). Thus, extra IOCs persist in *kibra* mutant clones as a result of decreased developmental apoptosis.

We assessed the proliferation rate of *kibra* mutant cells in imaginal discs, the larval precursors to the adult appendages. By using the FLP/FRT system under the control of the *heat-shock* promoter, *kibra* mutant cells and their WT sister clones were generated through single recombination events from heterozygous mother cells (Brumby and Richardson, 2005). After several rounds of divisions, the sizes of mutant clones (no GFP) and WT twin spots (two copies of GFP) were compared, allowing us to estimate the relative proliferation rates of mutant versus WT cells. The total *kibra* clone area is 1.57 (±0.12)-fold larger than the control twin spot area, compared to a ratio of 0.98 (±0.09) when both clones and twin spots are WT (Figures 1Q–1S), indicating that $kibra^{\Delta 32}$ mutant cells grow 1.6 times faster than WT cells.

In addition to cell cycle rates, the timing of cell cycle exit can readily be measured in the eye disc, where cell divisions follow a spatially determined pattern (Wolff and Ready, 1993). During the third larval instar, the morphogenetic furrow, a wave of

differentiation, sweeps the eye disc from posterior to anterior. Anterior to the furrow cells still proliferate asynchronously, while in the furrow cells synchronize in G1. Immediately posterior to the furrow, cells enter a final round of synchronous S phases, the second mitotic wave (SMW). Posterior to the SMW, most cells permanently exit the cell cycle. Thus, in WT discs, no S phases (marked by EdU incorporation) can be observed posterior to the SMW (Figure 1T). As expected, *hpo* mutant cells fail to exit from the cell cycle in a timely manner and present ectopic EdU-positive staining posterior to the SWM (Figures S1B and S1B′). *kibra* mutant cells exhibit a less pronounced but similar phenotype (Figures 1U and 1V). Thus, *kibra* mutant tissues have a proliferative advantage and an apoptosis defect, consistent with an involvement in the SWH network. The overgrowth defect appears more subtle than that of core pathway members such as *wts* and is more akin to upstream regulators (e.g., *ex* and *mer*).

Kibra Regulates SWH Network Targets in Ovarian Posterior Follicle Cells

Several transcriptional targets of the SWH network have been identified, such as the *Drosophila Inhibitor of Apoptosis 1* (*DIAP1*) gene, the cell cycle regulator *cycE*, the miRNA *bantam,* as well as *ex* (Harvey and Tapon, 2007; Saucedo and Edgar, 2007). In *kibra* mutant wing or eye discs, we could not detect a strong change in DIAP1, CycE, or *ex-lacZ* reporter levels (data not shown). Since overgrowth of *kibra* mutant cells in the wing is subtle compared to *wts* mutants, it is possible that Kibra plays a relatively minor role in SWH signaling in the wing. Accordingly, using an anti-Kibra antibody we generated (Figures S2A–S2C), we noted that Kibra staining in the wing disc is weak and consists of a punctate apical staining which can clearly be observed when *kibra* is overexpressed in a stripe of cells. Thus, the extent to which Kibra is required may vary in different tissues.

We and others have previously reported that ovarian posterior follicle cells (PFCs) are particularly sensitive to SWH loss of function (Meignin et al., 2007; Polesello and Tapon, 2007; Yu et al., 2008), leading us to study the $kibra^{\Delta 32}$ phenotype in the ovary. First, we noted that Kibra protein levels are higher in follicle cells than in the wing discs (Figure S2D–S2E′). Kibra staining is mainly apical and is severely reduced in $kibra^{\Delta 32}$ clones. Similarly to *hpo* or *wts* loss of function, *kibra* loss of function in the PFCs induces an upregulation of the *ex-lacZ* reporter (Figures 2A–2B″, compare with Figures 2C–2C″). *hpo* or *wts* mutant PFCs also show a misregulation of the Notch (N) pathway and ectopic cell divisions (Meignin et al., 2007; Polesello and Tapon, 2007; Yu et al., 2008). The N target Hindsight (Hnt) is normally repressed in all follicle cells up to stage 6 and switched on from stage 7 to stage 10B (Figures 2D–2E″) (Poulton and Deng, 2007). Cut, which is repressed by Hnt, presents an opposite pattern of expression (Figures 2H–2I″). In *kibra* mutant PFCs from stage 7–10B egg chambers, Hnt expression is lost (Figures 2D–2D″ and 2F–2G″), while Cut is ectopically expressed (Figures 2J–2K″). This indicates that N signaling is downregulated in *kibra* mutant PFCs. Loss of *kibra* also leads to perturbation of epithelial integrity, as mutant PFCs show an accumulation of the apical polarity protein aPKC and the N receptor (Figures S2F–S2G″) as well as multilayering of the follicular epithelium (Figures 2I–2I″ and 2K–2K″). Ectopic mitotic divisions are also observed in PFCs clones after stage 6, as detected by phospho-histone H3 (PH3) staining (Figures S2H–S2H″). Together, these phenotypes are identical to those observed in *hpo* or *wts* loss of function, suggesting that Kibra is indeed a member of the SWH network.

Genetic Experiments Place *kibra* Upstream of the Core SWH Kinase Cassette

To further explore the role of Kibra in the SWH network, genetic interaction and epistasis experiments were performed. Overexpressing *kibra* in the eye under the *GMR (Glass Multimer Reporter)* promoter elicits the formation of a small rough eye with frequent ommatidial fusions (Figures S3A–S3B′). This phenotype can be partially rescued by removing one copy of the *hpo* gene (Figures S3C and S3C′). In contrast, overexpressing *kibra* could not rescue the *hpo*-like overgrowth phenotype induced by *yki* overexpression (Figures S3D and S3E), suggesting that Kibra may be an upstream regulator of the pathway.

To conduct epistasis experiments between *kibra* and *yki*, we used the MARCM system to generate clones of mutant cells while simultaneously overexpressing or depleting other pathway components (Lee and Luo, 1999). MARCM clones expressing *yki* RNAi generated with *eyFLP* lead to the formation of a normal eye, because *yki*-depleted cells are eliminated by apoptosis (data not shown) and replaced by WT cells (Figure S3F). As expected, *eyFLP kibra* MARCM clones cause eye overgrowth (Figure S3G). This overgrowth is rescued by *yki* depletion in the mutant cells (Figure S3H), indicating that the *kibra* overgrowth phenotype is *yki* dependent. Furthermore, overexpressing *kibra* in the eye under the *GMR* promoter induces apoptosis in third instar eye discs, which is suppressed by loss of *hpo* (Figures 3A–3A″). Together, these epistasis experiments are consistent with Kibra being a member of the SWH network acting upstream of Yki and Hpo.

Genetic interactions between *kibra*, *mer*, and *ex*, upstream members of the SWH network, were then investigated. Expressing a *kibra*, an *ex,* or a *mer* RNAi line in the eye under the *GMR* promoter induces eye overgrowth (Figures S3I–S3L). Combined depletion of either Ex/Kibra or Mer/Kibra shows stronger phenotypes than individual depletion of these proteins (Figures S3M and S3N). We used the MARCM technique to evaluate epistatic relationships between those three genes. *hsFLP* MARCM clones of various genotypes were generated and scored according to the severity of the wing overgrowth phenotypes, with type 0 representing normal wings and type 4 the strongest overgrowth (Figures 3B and 3C). Overexpressing *ex* or *mer* in *kibra* mutant clones significantly rescues the overgrowth of *kibra* mutant clones ($p < 0.0001$ for both genotypes). Reciprocally, *kibra* overexpression was also able to suppress the *ex* overgrowth phenotype ($p < 0.0001$). Thus, we could not determine a strict epistatic relationship between *kibra*, *ex*, and *mer*, consistent with a model whereby *kibra*, *ex*, and *mer* cooperate to control SWH pathway activity.

Kibra Is a Transcriptional Target of the SWH Network and Colocalizes with Mer and Ex

As well as being an upstream regulator of the SWH network, *ex* is also one of its transcriptional targets (Hamaratoglu et al., 2006), as are other upstream regulators (e.g., *mer*, *four-jointed*,

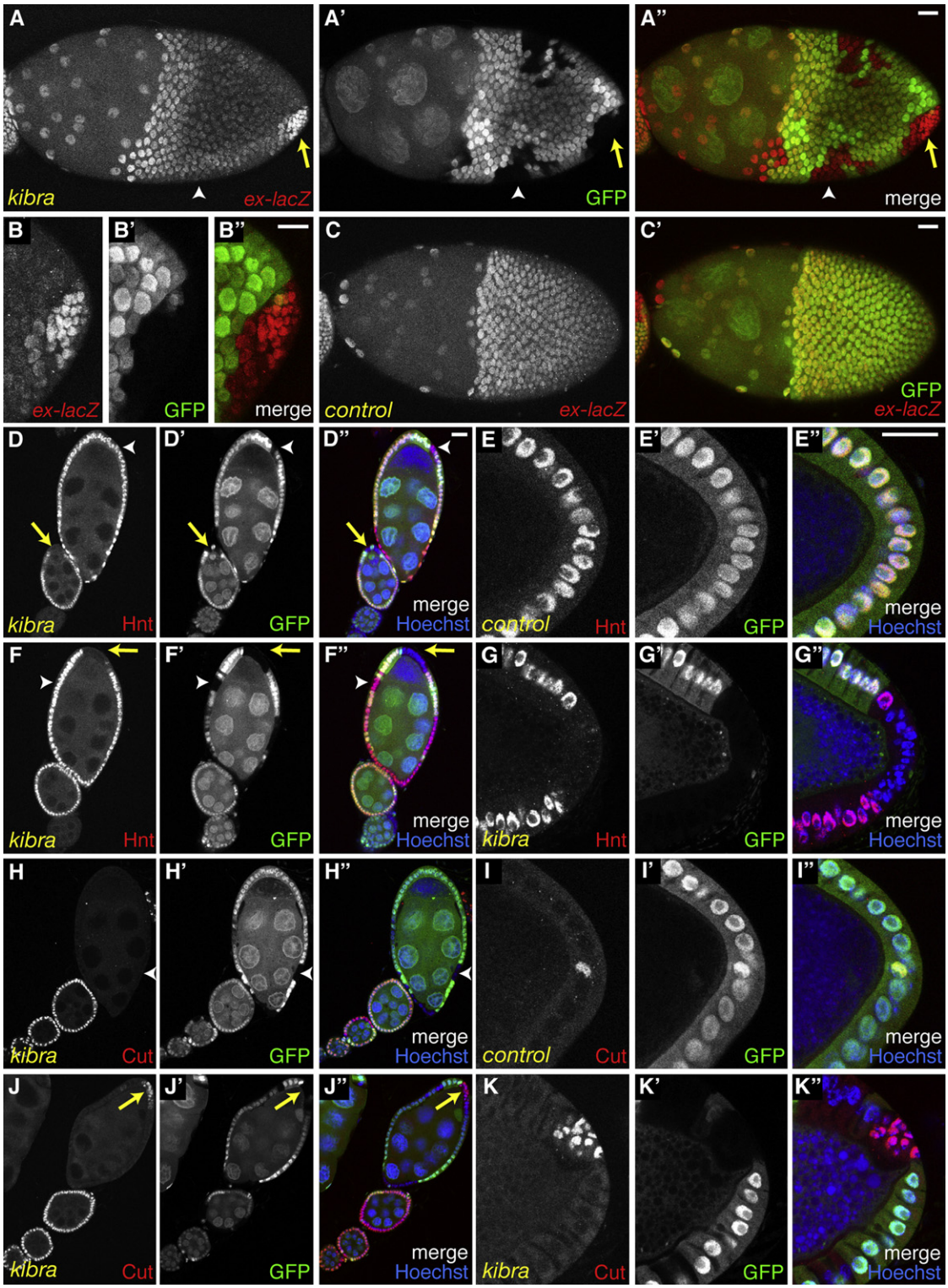

Figure 2. Kibra Regulates SWH Pathway Targets in Ovarian Posterior Follicle Cells

Egg chambers containing heat-shock-induced *kibra* mutant clones (absence of GFP). Yellow arrows point to *kibra* mutant cells in the PFC region while white arrowheads point to *kibra* cells in lateral follicle cells. Scale bars = 20 μm. (A–C′) Stage 10B egg chambers stained for β-galactosidase (gray or red), which monitors the activity of the *ex-lacZ* reporter. (B–B″) Close-up of the PFC region in (A)–(A″). (D–K″) Egg chambers stained for the N target Hindsight (Hnt) (D–G″) or for Cut (H–K″). Nuclei are shown in blue (Hoechst). (E)–(E″), (G)–(G″), (I)–(I″), and (K)–(K″) are close-ups of the PFC region of stage 10B egg chambers. (D–D″) The arrow points to a stage 8 clone; the arrowhead points to a stage 9 clone. (F–F″ and J–J″) Arrows and arrowheads point to clones in stage 9 egg chambers. See also Figure S2.

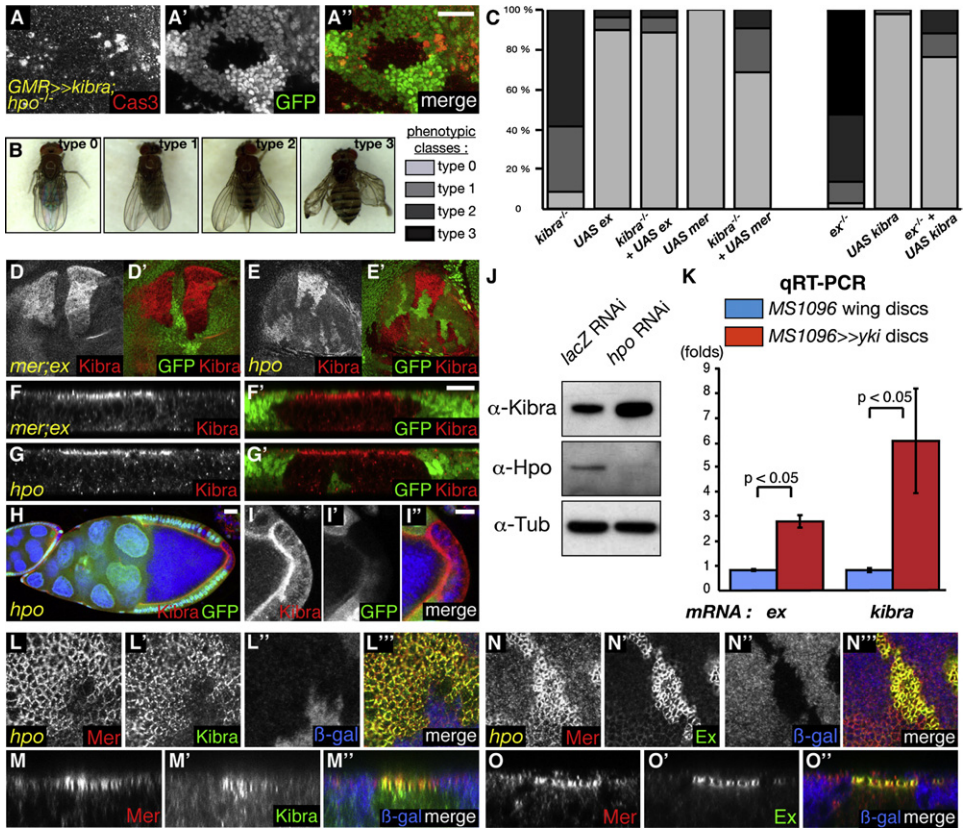

Figure 3. *kibra* Is Epistatic to *hpo* and Is a Transcriptional Target of the SWH Network

(A–A″) Third instar eye imaginal disc expressing *kibra* under the *GMR* promoter and containing *hpo* mutant cells (absence of GFP). Apoptosis is visualized by an anti-activated Caspase-3 staining. Posterior is to the bottom.

(B and C) Epistatic relationships between Kibra, Mer and Ex. Examples of the 4 phenotypic classes used to score are shown in (B). The percentages of each class for each genotype are summarized in (C).

(D–G′) Third instar imaginal discs containing clones (marked by absence of GFP) of cells mutant for *mer;ex* (D, D′, F, and F′) or *hpo* (E, E′, G, and G′). (D)–(E′) are XY sections while (F)–(G′) are XZ transverse sections (apical is to the top).

(H–I″) Stage 10A egg chamber containing a *hpo* clone (marked by absence of GFP) in the PFCs and stained for Kibra (red). (I)–(I″) show a higher magnification of the PFC region in (H). Nuclei are stained with Hoechst (blue). Scale bars = 20 μm (A–A″, D–E′, and H), 10 μm (F–G′ and I–I″).

(J) Lysates from S2R+ cells treated with *lacZ* RNAi or *hpo* RNAi and probed for Kibra and Tubulin.

(K) A graph presenting a comparison of *kibra* and *ex* mRNA levels between *yki* overexpressing and WT wing discs, as measured by qRT-PCR, is shown. p values from Mann-Whitney tests are shown. Error bars represent standard deviations.

(L–O″) XY and transverse sections of third instar imaginal wing discs containing *hpo* mutant clones (labeled by absence of βgal) and stained for Kibra (L–L″ and N–N″), Ex (M–M″ and O–O″), and Mer (L–O″). See also Figure S3.

dachsous). Since epistasis experiments place Kibra at the level of Mer and Ex, we wished to test whether this is also the case for *kibra*. Kibra levels were highly upregulated in *mer;ex* or *hpo* clones (Figures 3D–3E′), showing an apical localization (Figures 3F–3G′). The same is true in *hpo* clones in follicle cells (Figures 3H–3I″). Similarly, *hpo*-depleted cultured *Drosophila* S2R+ cells have increased Kibra levels (Figure 3J). To determine whether *kibra* is a transcriptional SWH network target, quantitative RT-PCR experiments were performed on *yki*-overexpressing and control wing imaginal discs (Figure 3K). As expected, *ex* mRNA levels were increased (2.97 ± 0.25-fold) in *yki*-expressing discs compared to control discs. Interestingly, *kibra* mRNA levels were also upregulated in *yki*-expressing discs (6.24 ± 2.12-fold), confirming that *kibra* is a Yki transcriptional target and suggesting the existence of a possible negative feedback loop regulating Kibra expression.

Because *hpo* clones present increased levels of Kibra as well as Mer and Ex, these constitute a good system to evaluate the colocalization of those proteins. Indeed, Kibra colocalizes with Mer in the wing disc (Figures 3L–3M″). As expected, Mer and Ex also colocalize (Figures 3N–3O″). Thus, Kibra, Mer, and Ex colocalize apically in imaginal disc cells, but are dispensable for each other's apical sorting, because Kibra is still apical in *mer;ex* clones and Mer/Ex are normally localized in *kibra* clones (Figures 3D, 3D′, 3F, and 3F′ and data not shown).

Kibra Associates with Ex and Mer, and the Kibra/Mer Complex Is Conserved in Human Cells

Because Kibra colocalizes with Mer/Ex, a possible association between those proteins was examined by conducting coimmunoprecipitation (co-IP) assays in S2R+ cells. Kibra was found to co-IP with Ex and Mer, but not with Hpo or with the negative

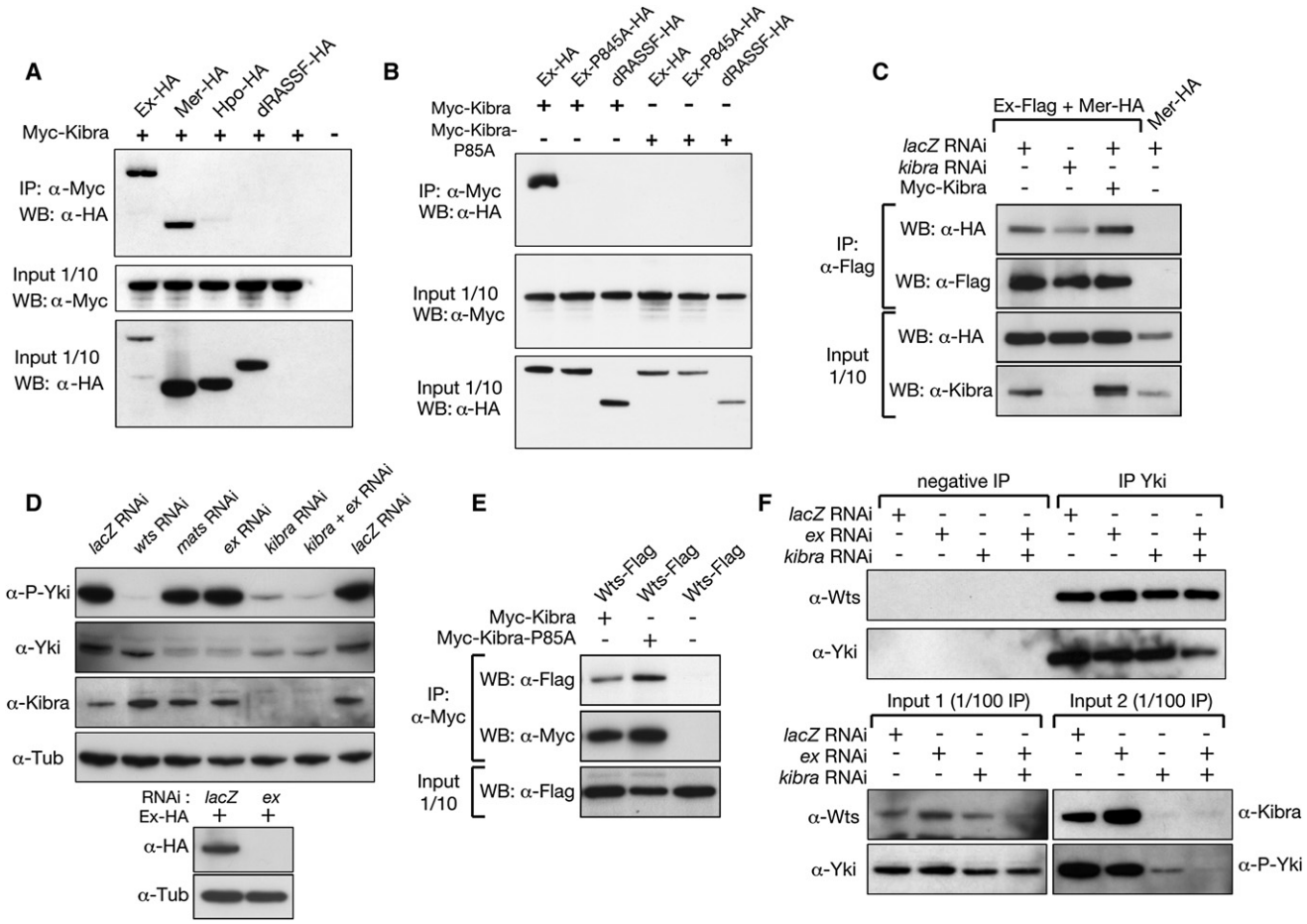

Figure 4. Kibra Associates with Mer and Ex, and *kibra* Depletion Strongly Reduces Yki Phosphorylation without Interfering with the Yki/Wts Interaction

(A and B) Western blots of coimmunoprecipitation assays between Myc-Kibra and HA-tagged members of the SWH network are shown.

(C) Western blots of co-IP assays between Mer-HA and Ex-Flag in presence or absence of Kibra are shown.

(D) Lysates of S2R+ cells treated with RNAi against different members of the SWH network and probed for P-Ser168 Yki (P-Yki), pan-Yki, Kibra, and Tubulin are shown (the anti-Kibra blot was performed on a parallel run of the same samples). The bottom panel shows efficiency of the *ex* dsRNAi treatment.

(E) Western blots of co-IP assays between Wts-Flag and different versions of Myc-tagged Kibra are shown.

(F) Endogenous co-IP assays between Yki and Wts in control S2 cells and in cells treated with *ex* and/or *kibra* RNAi are shown. The anti-Wts input blot was performed on a parallel run of the same samples. See also Figure S4.

regulator of Hpo, dRASSF (Polesello et al., 2006) (Figure 4A). Interestingly, Kibra was reported to interact with Mer in a large-scale yeast two-hybrid screening study (Formstecher et al., 2005). Kibra possesses two WW domains, which are predicted to mediate protein-protein interactions by binding to PPXY motifs. Furthermore, the first WW domain of human KIBRA was shown to recognize the consensus motif RXPPXY in vitro (Kremerskothen et al., 2003). In flies, Mer does not contain any PPXY sites, while Ex has two PPXY sites (P^{786}PPY and P^{1203}PPY) and an RXPPXY site (R^{842}DPPPY). We therefore further investigated the association between Kibra and Ex by mutating amino acids that are known to be required for WW domains and PPXY sites to interact (Kremerskothen et al., 2003; Otte et al., 2003). A Kibra protein mutant for its first WW domain (P85A) could no longer co-IP WT Ex. Reciprocally, WT Kibra could not co-IP an Ex protein deficient for its RXPPXY site (P845A) (Figure 4B). Thus, Kibra associates with Ex through its first WW domain and the Ex RXPPXY motif.

In contrast, mutating either one or both Kibra WW domains does not affect Kibra/Mer association (Figure S4A). Further assays reveal that both Kibra N- and C-terminal fragments are sufficient for the association with Mer, but a central stretch (aa 484–857) is not (Figure S4A). Because the WW motifs, which are required for the Ex/Kibra association, are located in the N-terminal fragment, this suggests that Mer can complex with Kibra both through Ex and independently of Ex. To further test this possibility, coimmunoprecipitation assays between Mer and Kibra were performed in *ex*-depleted cells (Figure S4B). The Kibra/Mer immunoprecipitation is not affected by *ex* depletion, suggesting that Ex is not required for the Kibra/Mer association.

Because the Hpo pathway is highly conserved from *Drosophila* to humans, we tested for potential interactions

between human KIBRA and the human orthologs of Ex (FRMD6), Mer (NF2/MER), Hpo (MST2), and dRASSF (RASSF6). We used split-TEV as readout, which is based on TEV protease complementation and represents a sensitive method for detecting interactions between membrane-associated proteins (Wehr et al., 2006, 2008). We found that KIBRA associates with NF2/MER but did not interact with FRMD6, MST2, or RASSF6 (Figure S4C). Interestingly, FRMD6 contains only an N-terminally conserved sequence of Ex but lacks the entire C-terminal part, which in Ex harbors the PPXY motifs. Thus, the missing PPXY motifs and the generally limited level of sequence conservation in FRMD6 likely explain the absence of interaction between KIBRA and FRMD6. These results imply that the ability to associate with Kibra evolved in an ancestral Ex/Mer-like FERM domain protein and was later lost in FRMD6 but retained in NF2/MER. Alternatively, an Ex functional homolog other than FRMD6 may exist.

As Kibra complexes with both Ex and Mer and Ex/Mer have been reported to directly interact (McCartney et al., 2000), we tested the possibility that Kibra could affect the Mer/Ex interaction. We performed co-IP assays between Mer and Ex in cells expressing different levels of Kibra protein (Figure 4C). The Mer/Ex interaction is reduced in *kibra*-depleted cells compared to WT cells, whereas the interaction is strengthened in cells that express a Myc-Kibra construct. Thus, the presence of Kibra is required to fine-tune the stability of the Mer/Ex interaction.

Kibra Associates with Wts and Is Required for Yki Phosphorylation, but Not for Yki/Wts Binding

Because Kibra complexes with Ex and a Yki/Ex interaction has recently been described (Badouel et al., 2009), we sought to determine whether Kibra can affect Yki activity. S2R+ cells were treated with RNAi against several SWH pathway components, and Yki phophorylation on Ser168 was monitored by western blotting (Figure 4D). The phosphorylation of Yki by Wts at Ser168 leads to Yki inactivation and sequestration in the cytoplasm, where it has been reported to bind Ex, Wts, Hpo, and 14.3.3 (Badouel et al., 2009; Huang et al., 2005; Oh and Irvine, 2008; Oh et al., 2009). *lacZ* RNAi-treated cells show a high basal level of phospho-Yki (P-Yki). As expected, Yki phosphorylation is abolished when Wts is depleted, and mildly reduced when the Wts cofactor Mats (Lai et al., 2005) is depleted. In *wts* treated RNAi cells, a Yki downward shift can also be observed using a pan-Yki antibody (Figure 4D, second row). *ex* RNAi treatment has only a mild effect on P-Yki levels. Interestingly, *kibra* depletion leads to a marked reduction in P-Yki. When depleted in conjunction with *ex*, the P-Yki signal becomes even further reduced.

This suggests that Kibra and Ex are required for Wts activity on Yki, which prompted us to investigate whether Kibra could associate with Wts. Co-IP assays reveal that Kibra interacts with Wts (Figure 4E). Wts does not seem to compete with Ex for Kibra association, because it could still complex with a form of Kibra mutant for its first WW domain. Because Kibra associates with Wts and Ex interacts with Yki, we investigated whether Wts requires Kibra/Ex to bind Yki. Endogenous IPs between Yki and Wts were performed in S2 cells treated with various dsRNAs (Figure 4F). In these conditions, the effect of *kibra* and *ex* depletion on Yki phosphorylation can also be observed (see input). In control cells, Wts binding to Yki is detected after immunoprecipitating Yki. This endogenous interaction is unaffected by the individual or combined depletion of *ex* and *kibra*. These results suggest that Ex and Kibra are required to activate the SWH pathway by nucleating an active Hpo/Wts kinase cassette, rather than promoting the Wts/Yki interaction.

DISCUSSION

Our data identify Kibra as a regulator of the SWH network that associates with Ex and Mer, with which it is colocalized apically and transcriptionally coregulated. Given that the apical surface of epithelial cells is instrumental in both cell-cell signaling and tissue morphogenesis, we speculate that Kibra may cooperate with Ex and Mer to transduce an extracellular signal, or relay information about epithelial architecture, via the SWH network, to control tissue growth and morphogenesis.

Recent data have suggested that an apical scaffold machinery containing Hpo, Wts, and Ex recruits Yki to the apical membrane, facilitating its inhibitory phosphorylation by Wts (Badouel et al., 2009; Oh et al., 2009). Since Kibra associates with Ex and is also apically localized, we can hypothesize that Kibra is also part of this scaffold and participates in nucleating an active Hpo/Wts complex and recruiting Yki for inactivation. This view is supported by our finding that Kibra complexes with Wts and that combined depletion of Kibra and Ex leads to a strong decrease in Yki phosphorylation, but does not disrupt the Wts/Yki interaction. Our data also suggest that the importance of Kibra may be tissue-specific since we observe robust phenotypes in ovaries and hemocyte-derived S2R+ cells, but weaker effects in imaginal discs. Thus, considering the relative levels of expression of Ex, Mer, and Kibra may be important in determining pathway activation. Finally, since mammalian KIBRA complexes with the NF2/MER tumor suppressor, our findings raise the possibility that human KIBRA may contribute to tumor suppression in human neurofibromas and potentially other tumors.

EXPERIMENTAL PROCEDURES

For *Drosophila* genotypes, primer sequences, and further experimental details, see Supplemental Experimental Procedures.

kibra Mutant

The P element of *EP747* (Bloomington stock center) was mobilized using standard genetic techniques, and excisions were screened by PCR (see Supplemental Experimental Procedures for details).

Immunostainings

Immunostainings and confocal image acquisitions were performed as in Genevet et al. (2009). Mouse β-galactosidase (Promega), rabbit anti-Cleaved Caspase-3 (Asp175) (Cell Signaling Technology), rabbit anti-aPKC (Santa Cruz), and mouse NICD (C17.9C6, Development Studies Hybridoma Bank) antibodies were used at 1/500. Mouse anti-Arm, anti-Cut, and anti-Hnt (N2 7A1, 2B10 and 1G9, DSHB) were used at 1/10 and 1/20. The EdU staining was performed as described in the Click-iT EdU Alexa Fluor Imaging Kit (Invitrogen). Guinea pig anti-Mer, a gift from R. Fehon, was used at 1/7500, and rabbit anti-Ex, a gift from A. Laughon, at 1/400. Rabbit anti-Kibra antibody (Kib18, 1/100) was generated by Eurogentec SA (Seraing, Belgium) against a peptide corresponding to the last 15 amino acids of Kibra.

Quantification of Apoptotic Indexes in Mutant Clones versus WT Tissue

Apoptotic indexes were quantified on 6 retinas as described in Colombani et al. (2006).

Standard Growth Conditions and Size Measurements

The experiment was performed as described in Genevet et al. (2009). Ten wing discs for each genotype were analyzed.

Fly Eye Scanning Electron Microscopy

Scanning microscopy of adult flies was performed as described in Polesello et al. (2006).

RNAi Treatment and Coimmunoprecipitation of Proteins

For RNAi treatment, S2 or S2R+ cells were treated with dsRNAs as indicated for 4 days. For coimmunoprecipitations, S2R+ or S2 cells transfected with the indicated plasmids were used. See Supplemental Experimental Procedures for details.

Quantitative RT-PCR

MS1096 > > (control) and *MS1096 > > yki* wing discs were dissected in PBS and snap-frozen in liquid nitrogen. RNA isolation and subsequent qRT-PCR reactions were performed as described in Genevet et al. (2009). See Supplemental Experimental Procedures for primer sequences.

Statistical Analysis

All error bars displayed represent standard deviations. All statistical analyses performed (except epistasis analysis) were assessed by Mann-Whitney nonparametric tests using the website http://elegans.swmed.edu/~leon/stats/utest.html.

The epistasis analysis was made by pairwise comparison after correction for the batch effect on 42 to 310 flies of each genotype, divided in 4 to 6 cohorts. The approach used was a three-way log-linear model, against a null-hypothesis of no interaction between phenotype and population. The p value indicates whether the pair of populations differ in their phenotype profiles: p value($kibra^{-/-}$; $kibra^{-/-}$ + *UAS ex*) = 2.69×10^{-63}, p value($kibra^{-/-}$; $kibra^{-/-}$ +*UAS mer*) = 6.07×10^{-35}, p value($ex^{-/-}$; $ex^{-/-}$ + *UAS kibra*) = 1.76×10^{-20}.

SUPPLEMENTAL INFORMATION

Supplemental Information includes four figures, Supplemental Experimental Procedures, and Supplemental References and can be found with this article online at doi:10.1016/j.devcel.2009.12.011.

ACKNOWLEDGMENTS

We thank D. Pan, R. Fehon, G. Halder, A. Laughon, K. Irvine, J. Kremerskothen, G. Struhl, T. Igaki, H. McNeill, the Bloomington and VDRC stock centres, and the DGRC for fly stocks and reagents. We are very grateful to G. Dietzl, B. Dickson, and S. Cohen for their support in carrying out the RNAi screen. We are grateful to K. Blight, A. Weston, and L. Collinson from the LRI Electron Microscopy Facility and to P. Jordan from the Light Microscopy Facility for technical help, to G. Kelly for help with statistics, to F. Josué for help with apoptotic index analysis, as well as to T. Gilbank, S. Murray, and S. Maloney from the Fly Facility for technical support. We thank S. Cohen and C. Polesello for discussions and comments on the manuscript. We thank H. Stocker and E. Hafen for discussing data prior to publication. M.C.W. is supported by an EMBO long-term fellowship. The Tapon and Thompson laboratories are supported by Cancer Research UK.

Received: May 27, 2009
Revised: October 20, 2009
Accepted: December 24, 2009
Published: February 15, 2010

REFERENCES

Badouel, C., Gardano, L., Amin, N., Garg, A., Rosenfeld, R., Le Bihan, T., and McNeill, H. (2009). The FERM-domain protein expanded regulates Hippo pathway activity via direct interactions with the transcriptional activator Yorkie. Dev. Cell *16*, 411–420.

Boutros, M., Kiger, A.A., Armknecht, S., Kerr, K., Hild, M., Koch, B., Haas, S.A., Paro, R., and Perrimon, N. (2004). Genome-wide RNAi analysis of growth and viability in Drosophila cells. Science *303*, 832–835.

Brumby, A.M., and Richardson, H.E. (2005). Using Drosophila melanogaster to map human cancer pathways. Nat. Rev. Cancer *5*, 626–639.

Buther, K., Plaas, C., Barnekow, A., and Kremerskothen, J. (2004). KIBRA is a novel substrate for protein kinase Czeta. Biochem. Biophys. Res. Commun. *317*, 703–707.

Colombani, J., Polesello, C., Josue, F., and Tapon, N. (2006). Dmp53 activates the Hippo pathway to promote cell death in response to DNA damage. Curr. Biol. *16*, 1453–1458.

Conlon, I., and Raff, M. (1999). Size control in animal development. Cell *96*, 235–244.

Dietzl, G., Chen, D., Schnorrer, F., Su, K.C., Barinova, Y., Fellner, M., Gasser, B., Kinsey, K., Oppel, S., Scheiblauer, S., et al. (2007). A genome-wide transgenic RNAi library for conditional gene inactivation in Drosophila. Nature *448*, 151–156.

Duning, K., Schurek, E.M., Schluter, M., Bayer, M., Reinhardt, H.C., Schwab, A., Schaefer, L., Benzing, T., Schermer, B., Saleem, M.A., et al. (2008). KIBRA modulates directional migration of podocytes. J. Am. Soc. Nephrol. *19*, 1891–1903.

Formstecher, E., Aresta, S., Collura, V., Hamburger, A., Meil, A., Trehin, A., Reverdy, C., Betin, V., Maire, S., Brun, C., et al. (2005). Protein interaction mapping: a Drosophila case study. Genome Res. *15*, 376–384.

Genevet, A., Polesello, C., Blight, K., Robertson, F., Collinson, L., Pichaud, F., and Tapon, N. (2009). The Hippo pathway regulates apical domain size independently of its growth control function. J. Cell Sci. *122*, 2360–2370.

Hamaratoglu, F., Willecke, M., Kango-Singh, M., Nolo, R., Hyun, E., Tao, C., Jafar-Nejad, H., and Halder, G. (2006). The tumour-suppressor genes NF2/Merlin and Expanded act through Hippo signalling to regulate cell proliferation and apoptosis. Nat. Cell Biol. *8*, 27–36.

Harvey, K., and Tapon, N. (2007). The Salvador-Warts-Hippo pathway—an emerging tumour-suppressor network. Nat. Rev. Cancer *7*, 182–191.

Huang, J., Wu, S., Barrera, J., Matthews, K., and Pan, D. (2005). The Hippo signaling pathway coordinately regulates cell proliferation and apoptosis by inactivating Yorkie, the *Drosophila* homolog of YAP. Cell *122*, 421–434.

Kango-Singh, M., Nolo, R., Tao, C., Verstreken, P., Hiesinger, P.R., Bellen, H.J., and Halder, G. (2002). Shar-pei mediates cell proliferation arrest during imaginal disc growth in Drosophila. Development *129*, 5719–5730.

Kremerskothen, J., Plaas, C., Buther, K., Finger, I., Veltel, S., Matanis, T., Liedtke, T., and Barnekow, A. (2003). Characterization of KIBRA, a novel WW domain-containing protein. Biochem. Biophys. Res. Commun. *300*, 862–867.

Lai, Z.C., Wei, X., Shimizu, T., Ramos, E., Rohrbaugh, M., Nikolaidis, N., Ho, L.L., and Li, Y. (2005). Control of cell proliferation and apoptosis by Mob as tumor suppressor, Mats. Cell *120*, 675–685.

Lee, T., and Luo, L. (1999). Mosaic analysis with a repressible cell marker for studies of gene function in neuronal morphogenesis. Neuron *22*, 451–461.

McCartney, B.M., Kulikauskas, R.M., LaJeunesse, D.R., and Fehon, R.G. (2000). The neurofibromatosis-2 homologue, Merlin, and the tumor suppressor expanded function together in Drosophila to regulate cell proliferation and differentiation. Development *127*, 1315–1324.

Meignin, C., Alvarez-Garcia, I., Davis, I., and Palacios, I.M. (2007). The Salvador-Warts-Hippo pathway is required for epithelial proliferation and axis specification in *Drosophila*. Curr. Biol. *17*, 1871–1878.

Muller, D., Kugler, S.J., Preiss, A., Maier, D., and Nagel, A.C. (2005). Genetic modifier screens on Hairless gain-of-function phenotypes reveal genes

involved in cell differentiation, cell growth and apoptosis in Drosophila melanogaster. Genetics *171*, 1137–1152.

Oh, H., and Irvine, K.D. (2008). In vivo regulation of Yorkie phosphorylation and localization. Development *135*, 1081–1088.

Oh, H., Reddy, B.V., and Irvine, K.D. (2009). Phosphorylation-independent repression of Yorkie in Fat-Hippo signaling. Dev. Biol. *335*, 188–197.

Otte, L., Wiedemann, U., Schlegel, B., Pires, J.R., Beyermann, M., Schmieder, P., Krause, G., Volkmer-Engert, R., Schneider-Mergener, J., and Oschkinat, H. (2003). WW domain sequence activity relationships identified using ligand recognition propensities of 42 WW domains. Protein Sci. *12*, 491–500.

Polesello, C., and Tapon, N. (2007). Salvador-warts-hippo signaling promotes *Drosophila* posterior follicle cell maturation downstream of Notch. Curr. Biol. *17*, 1864–1870.

Polesello, C., Huelsmann, S., Brown, N.H., and Tapon, N. (2006). The *Drosophila* RASSF homolog antagonizes the Hippo pathway. Curr. Biol. *16*, 2459–2465.

Poulton, J.S., and Deng, W.M. (2007). Cell-cell communication and axis specification in the Drosophila oocyte. Dev. Biol. *311*, 1–10.

Reddy, B.V., and Irvine, K.D. (2008). The Fat and Warts signaling pathways: new insights into their regulation, mechanism and conservation. Development *135*, 2827–2838.

Ringrose, L., Rehmsmeier, M., Dura, J.M., and Paro, R. (2003). Genome-wide prediction of Polycomb/Trithorax response elements in *Drosophila* melanogaster. Dev. Cell *5*, 759–771.

Rosse, C., Formstecher, E., Boeckeler, K., Zhao, Y., Kremerskothen, J., White, M.D., Camonis, J.H., and Parker, P.J. (2009). An aPKC-exocyst complex controls paxillin phosphorylation and migration through localised JNK1 activation. PLoS Biol. *7*, e1000235.

Saucedo, L.J., and Edgar, B.A. (2007). Filling out the Hippo pathway. Nat. Rev. Mol. Cell Biol. *8*, 613–621.

Tapon, N., Harvey, K.F., Bell, D.W., Wahrer, D.C., Schiripo, T.A., Haber, D.A., and Hariharan, I.K. (2002). *salvador* promotes both cell cycle exit and apoptosis in Drosophila and is mutated in human cancer cell lines. Cell *110*, 467–478.

Tseng, A.S., and Hariharan, I.K. (2002). An overexpression screen in Drosophila for genes that restrict growth or cell-cycle progression in the developing eye. Genetics *162*, 229–243.

Wehr, M.C., Laage, R., Bolz, U., Fischer, T.M., Grunewald, S., Scheek, S., Bach, A., Nave, K.A., and Rossner, M.J. (2006). Monitoring regulated protein-protein interactions using split TEV. Nat. Methods *3*, 985–993.

Wehr, M.C., Reinecke, L., Botvinnik, A., and Rossner, M.J. (2008). Analysis of transient phosphorylation-dependent protein-protein interactions in living mammalian cells using split-TEV. BMC Biotechnol. *8*, 55.

Wolff, T., and Ready, D.F. (1993). Pattern formation in the *Drosophila* retina. In The Development of *Drosophila melanogaster*, *Volume 2*, M. Bate and A.M. Arias, eds. (Cold Spring Harbor, NY: Cold Spring Harbor Laboratory Press).

Yu, J., Poulton, J., Huang, Y.C., and Deng, W.M. (2008). The hippo pathway promotes Notch signaling in regulation of cell differentiation, proliferation, and oocyte polarity. PLoS ONE *3*, e1761.